

## CHAPTER 4

### PETROGRAPHIC, GEOCHEMICAL AND GEOCHRONOLOGICAL DATA FOR EYJAFJÖLL

#### Stratigraphy

Some fifty-seven rock samples were taken from the Eyjafjöll Volcanic System for this study. These samples come from all regions of the system and are believed to represent the entire age and compositional range present. Figure 4.01 shows the geographical distribution of the samples and the grouping of these into ten distinct sections. Beginning in the northernmost region of the system and moving counter-clockwise around the central glacier, Eyjafjölljökull, these are: Merkurker, Sauðá (2); Kambagil (1); Seljalandsheiði (13); Hvamsmúli (9); Asólfsskálaegg (3); Steinafjall (16); Lambafellsheiði (5); Raufarfell (1); Skogaheiði (4); and 'top of mountain till' (3) (numbers in parentheses are the number of samples taken from each section). Figure 4.02 shows the corresponding geology, modified after maps done by Jónsson (1988), and Jakobsson (1979).

The Eyjafjöll Volcanic System is made up of interlayered hyaloclastite beds and lava flows. Only one hyaloclastite was sampled, Ey-33. The rest of the samples were all taken from the lava flows and sills. Table 4.01 shows the relative stratigraphical relationships within the ten sampling sections as inferred from field evidence and K-Ar dating. (Note: these are not real cross-sections, as material may, and often does exist between samples. This unsampled material consists of hyaloclastites, sedimentary beds, and other flows.) More detailed cross-sections of Steinafjall and Hvamsmúli were prepared in the field during the 1990 summer field season by Dr. Robert Duncan and Dr. Shaul Levi. The data from these sections have been added to data

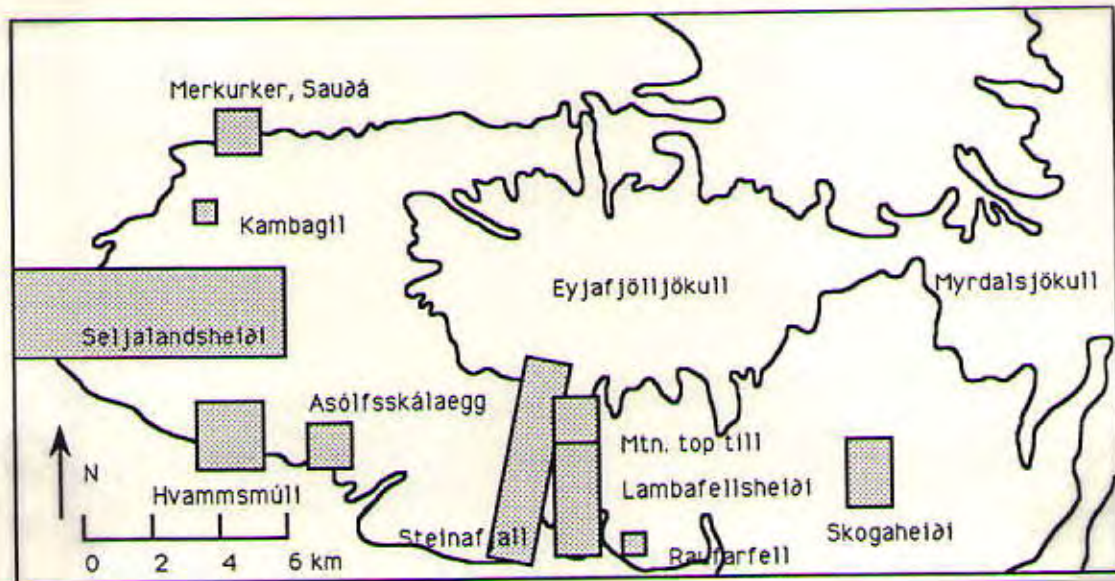


**Figure 4.01:** Eyjafjöll Volcanic System. Hatchured fields represent sampling sections.



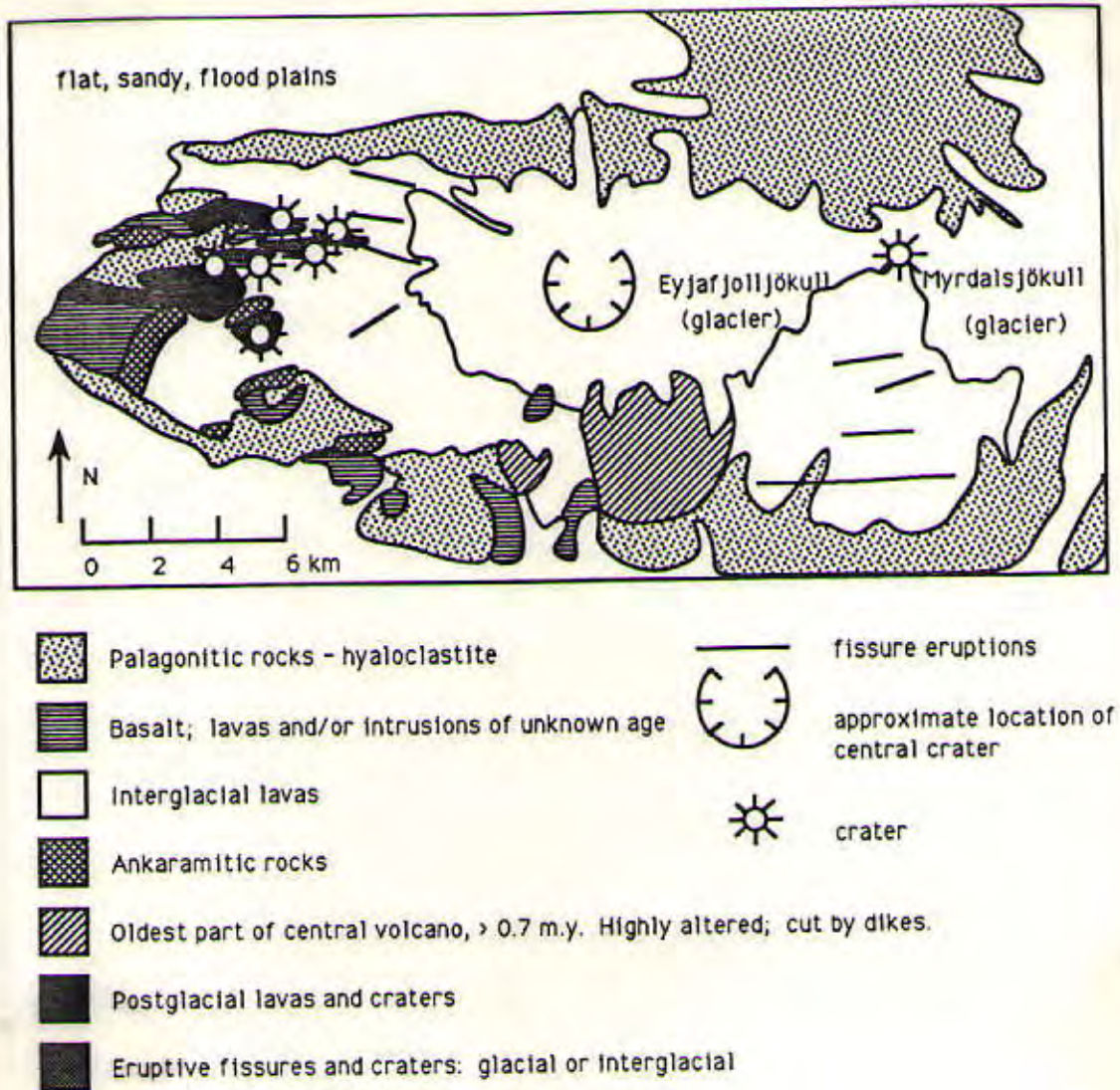


**Figure 4.02:** Eyjafjöll Volcanic System - Geology (modified from Jakobsson, 1979, and Jón Jónsson, 1988 ). Summit is at 1668 meters; base is at sea level.

**Table 4.01: Eyjafjöll stratigraphy.**

Solid lines indicate relative position in field. (ages in Ka)

<b>Merkurker, Sauðá</b>		<u>Ey-43 - stream float</u>
	149±24	<u>Ey-44 - intrusion at base of section</u>

<b>Kambagil</b>		<u>Ey-55 - holocene flow</u>
-----------------	--	------------------------------

<b>Seljalandsheiði</b>	<i>postglacial</i>	Ey-4A, Ey-4B, Ey-42 - flow
	<i>postglacial</i>	Ey-37, Ey-36 - cone intrusions
	Canyon north of cone	Ridge west of cone
	<u>Ey-39</u>	<u>Ey-40</u>
58±18	<u>Ey-38</u>	<u>Ey-41</u>
	Quarry - southwest of postglacial activity	
		Ey-33 - hyaloclastite
39±10		Ey-34 - intrusion
82±21		Ey-2 - flow south of quarry
76±45		Ey-3 - flow

<b>Hvammsmúll</b>		<u>Ey-53</u>
	349±19	<u>Ey-52</u>
	619±26	<u>Ey-20</u>
	589±37	<u>Ey-19</u>
		<u>Ey-18</u>
		<u>Ey-17, Ey-32</u>
	587±31	<u>Ey-1</u>

<b>Asólfsskálaegg</b>	129±20	<u>Ey-50</u>
		<u>Ey-49</u>
Ey-54 - west of section	121±39	<u>Ey-48</u>

<b>Steinafjall</b>	116±20	<u>Ey-27</u>
		<u>Ey-30</u>
	394±25	<u>Ey-13</u>
	309±18	<u>Ey-14</u>
		<u>Ey-15</u>
	414±21	<u>Ey-12</u>
	706±11	<u>Ey-11</u>
	<857±17>	<u>Ey-16 - sill (unreliable date)</u>
		<u>Ey-10</u>
	709±32	<u>Ey-9</u>
	797±17	<u>Ey-8</u> STF-3 - not in place
	702±17	<u>Ey-7, STF-1</u>
	722±33	<u>Ey-6</u>
	809±50	<u>Ey-5</u>
	<780±30>	McDougall (in Kristjansson et al., 1988)



Table 4.01 continued: Eyjafjoll stratigraphy.

Solid lines indicate relative position in field. (ages in Ka)

Lambafellsheiði	<u>Ey-26</u>	Hotsprings to the east
31±28	<u>Ey-24</u>	87±16 Ey-23, Ey-22
54±15	Ey-31	

Raufarfell	Ey-47
------------	-------

Skogaheiði	18±16	<u>Ey-45, Ey-46</u>
	118±34	STF-5 Ey-21

Top of mountain till	Ey-29, Ey-28, Ey-25
----------------------	---------------------

from work done by Steinhórsson (1964) at Hvammsmúli, and Kristjánsson et al. (1988) at Steinafjall. The modified sections are shown in Figures 4.03 and 4.04.

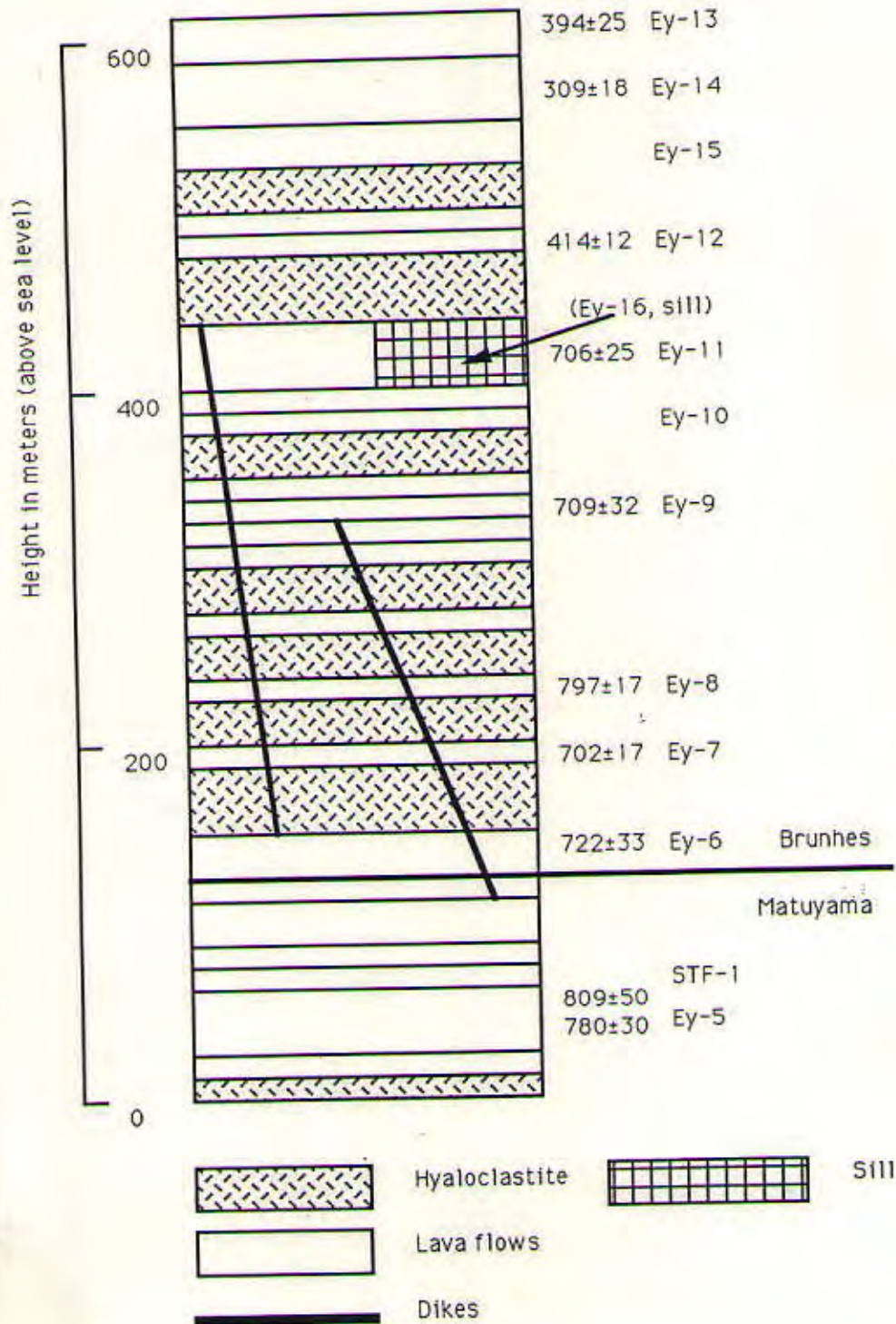
The stratigraphy displays a number of age gaps within certain sections, as well as system-wide. Between approximately 425-575 m.y. (435 min to 552 max), and 150-300 m.y. (173 min to 281 max) there are no data. Often this age gap corresponds to large hyaloclastite layers as seen in the previous two cross-section figures. These gaps will be discussed in more detail in the next chapter.

Flow thickness was estimated in the field, and this is given with the hand-sample descriptions in Appendix A. There is a range from thin flows of 1-2 meters thickness to large flows > 50 meters thick. Volumes could not be determined, as most outcrops were in the sides of cliffs and allowed for only a two-dimensional view. Also, much of the material has been eroded away during past glacial events.

#### Major and Trace Element Data






Major element and most trace element data were collected by XRF analysis as discussed in Chapter 3. They are listed in full in Appendix B, followed by CIPW norm calculations and equilibrium olivine calculations (Roeder and Emslie, 1970); only the normalized major element data were used. Major element oxide plots are shown in Figure 4.05(a-h), and trace elements are shown in Figure 4.05(i-m). The high Mg rocks, Ey-1, Ey-17, Ey-49, and STF-3 have been referred to by previous investigators (Steinhórsson, 1964; Jónsson, 1988) as ankaramites and in fact Ey-1 comes from the type locality for ankaramites. These samples are labeled as cumulates in the variation diagrams and will be discussed further in the next section.



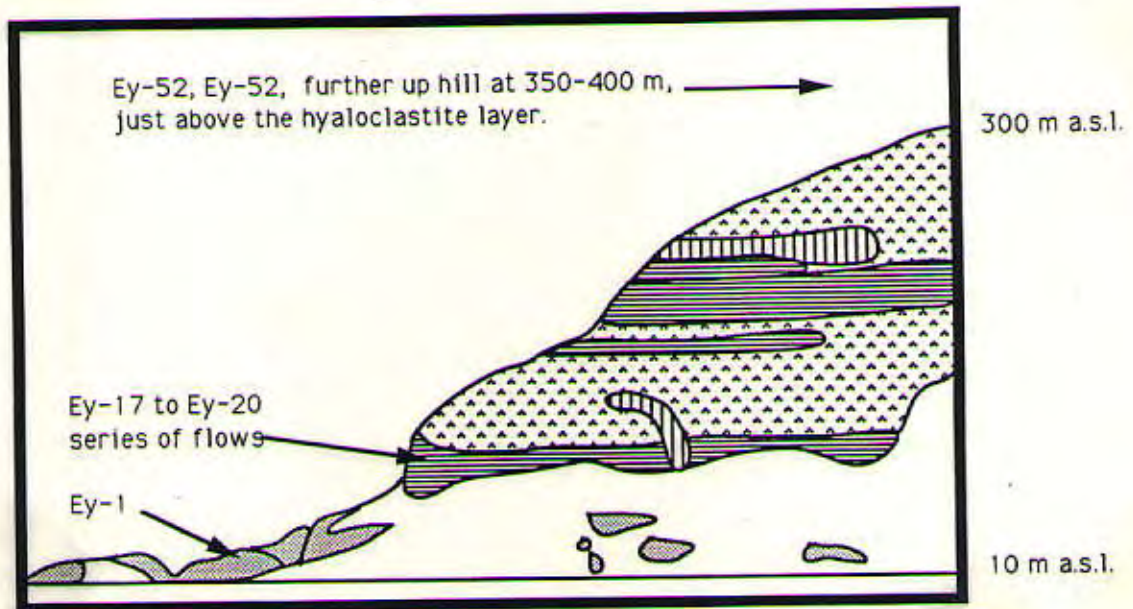


**Figure 4.03:** Approximate stratigraphy of lowest portion of Steinafjall sampling section. Data are from field work of Duncan and Levi in 1991 compiled with data from Kristjánsson et al. (1988). Thicknesses are approximated. Ages in Ka.



-  Hyaloclastites
-  Scree and soil cover
-  Ankaramites, examined in detail by Steinthorsson, 1964
-  Sills and lava flows
-  Veins and dykes

**Figure 4.04:** Geological cross-section of Hvammsmúli from the East, from Steinthórsson (1964). Horizontal distance is 0.5 km.



**Figure 4.05 (a-m):** Major (a-h) and trace (i-m) element variation diagrams, with data for the Eyjafjöll Volcanic System. Cumulates indicate the four samples referred to in the text as ankaramites and picrites.

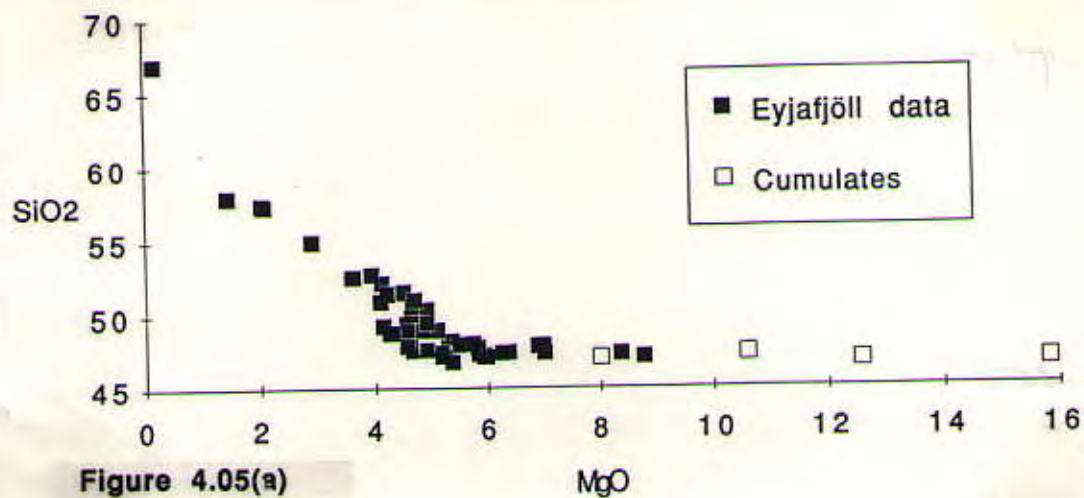


Figure 4.05(a)

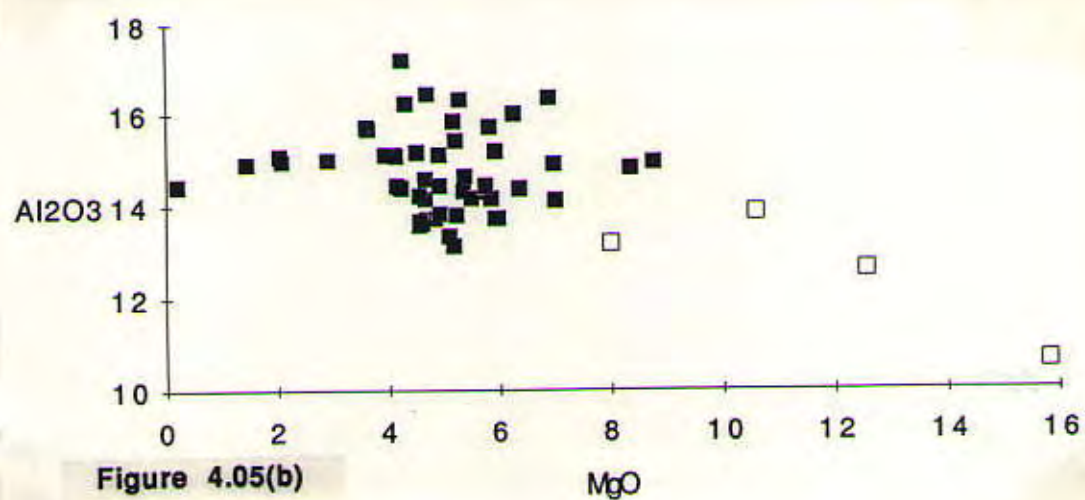


Figure 4.05(b)

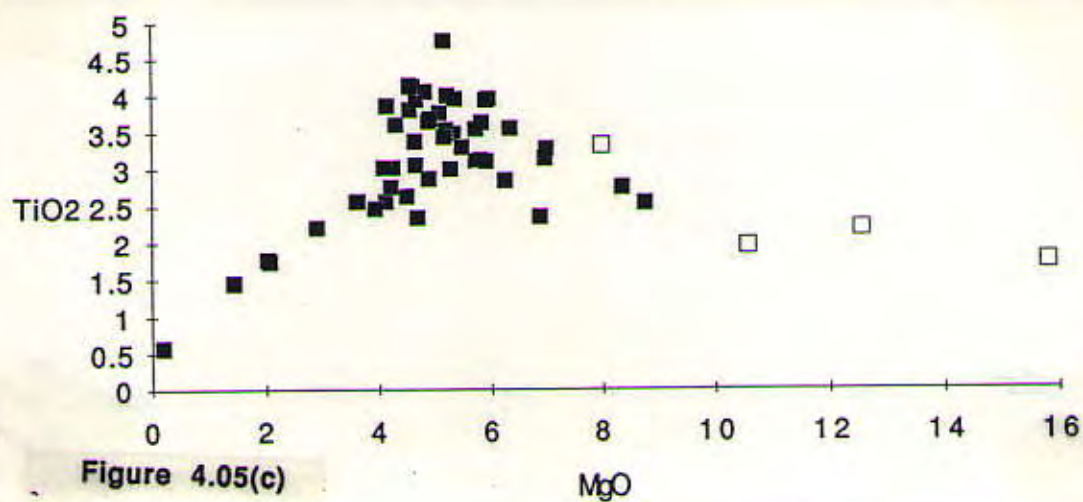


Figure 4.05(c)



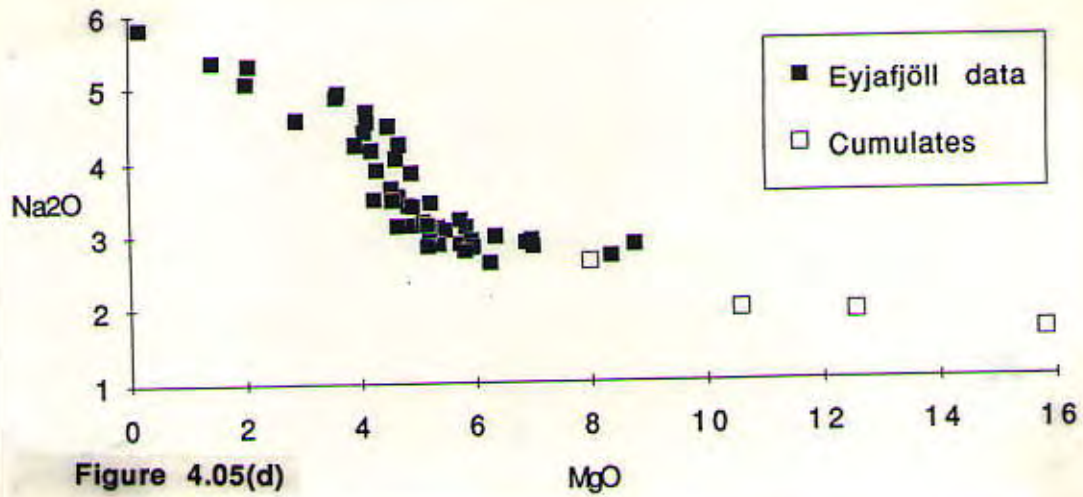


Figure 4.05(d)

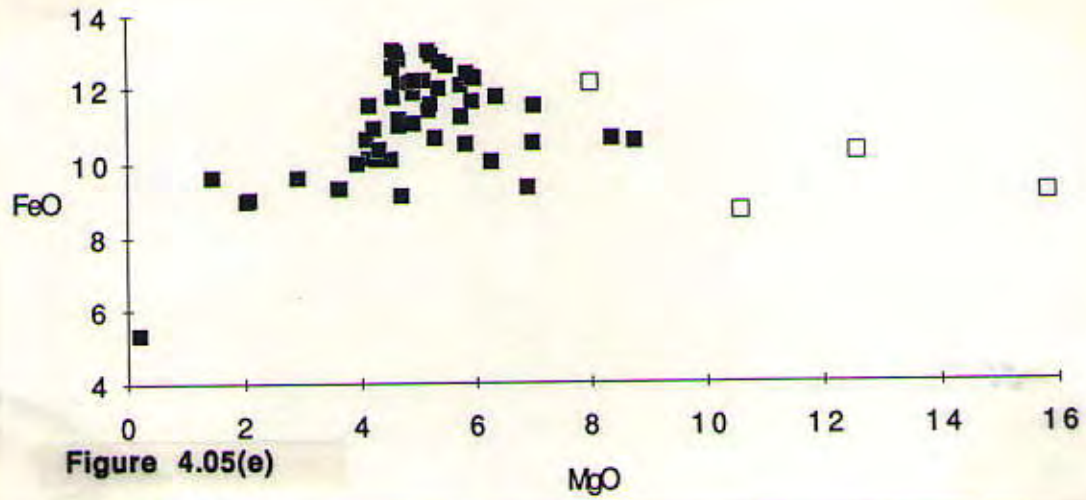


Figure 4.05(e)

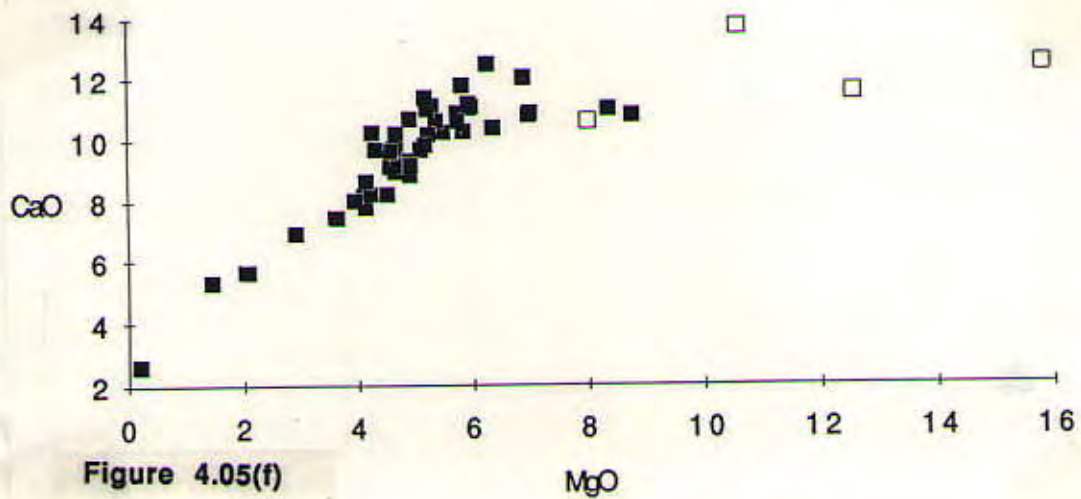
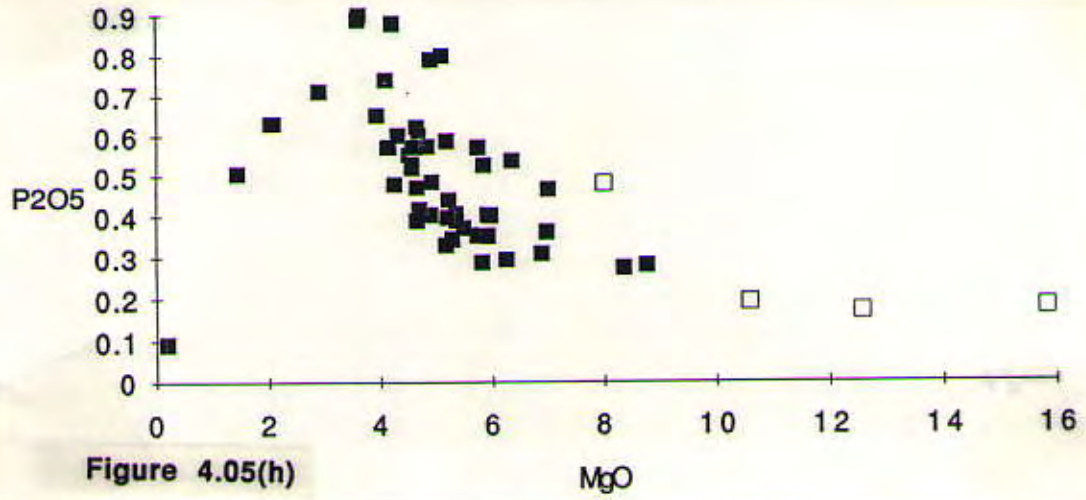
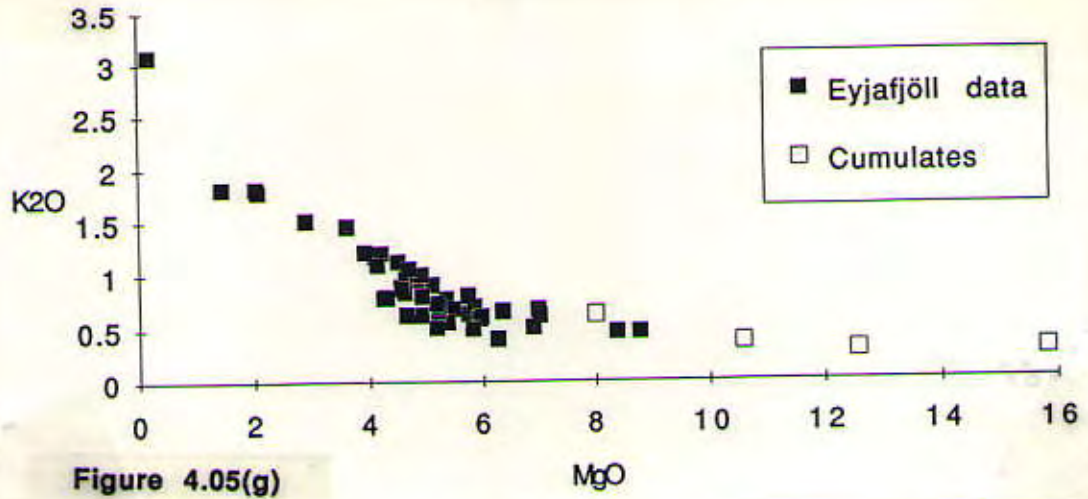


Figure 4.05(f)





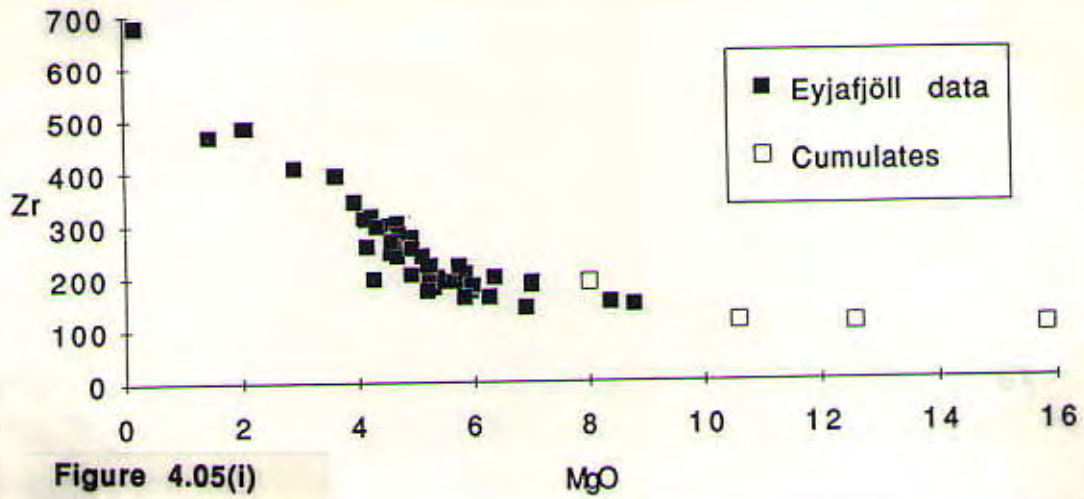


Figure 4.05(i)

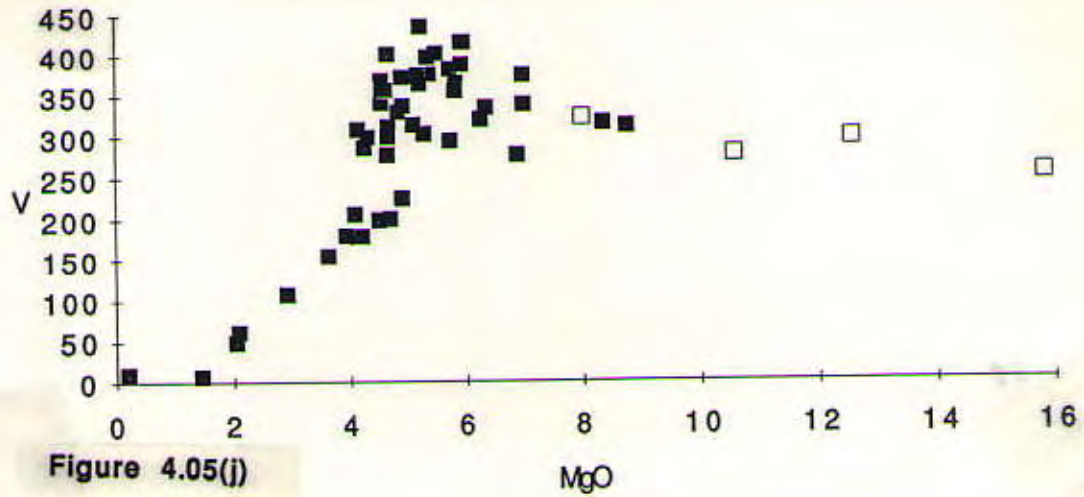


Figure 4.05(j)

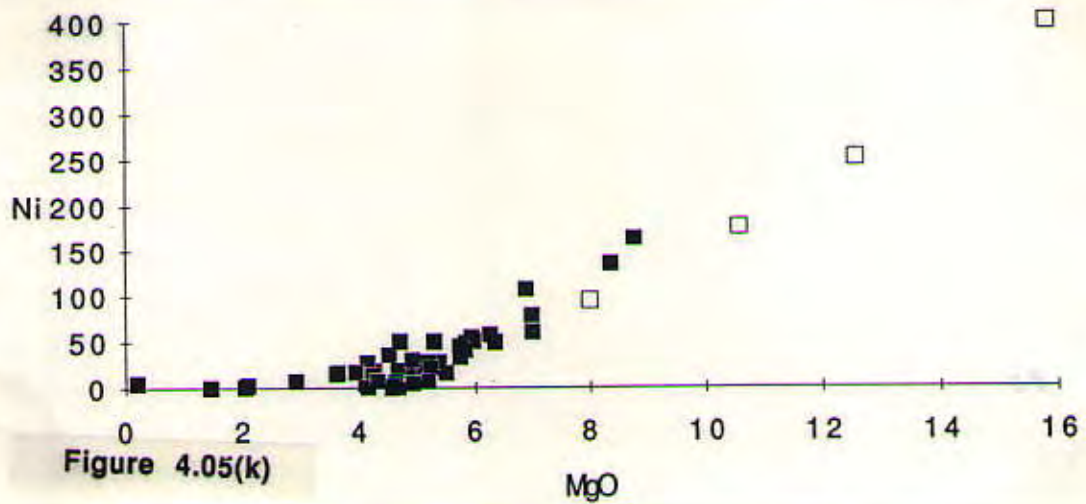
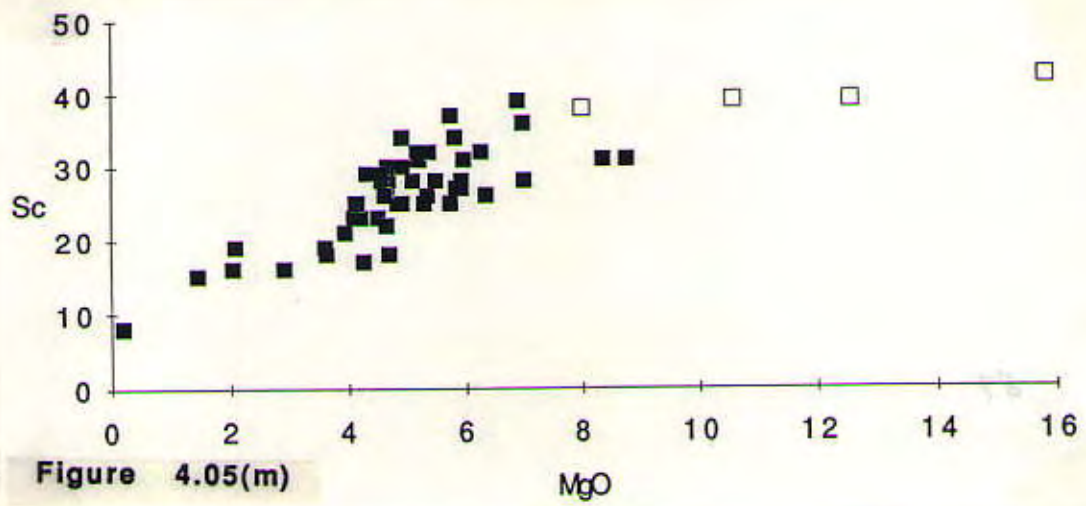
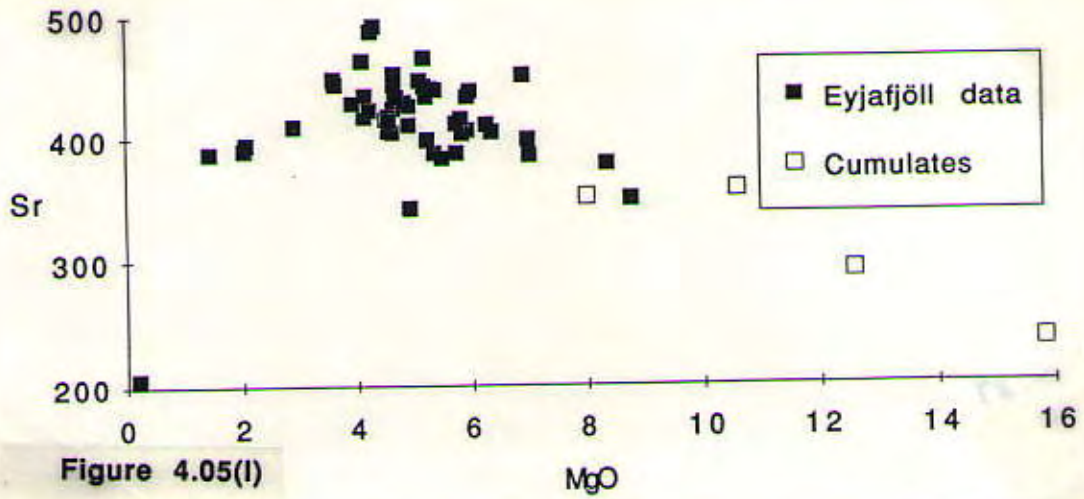
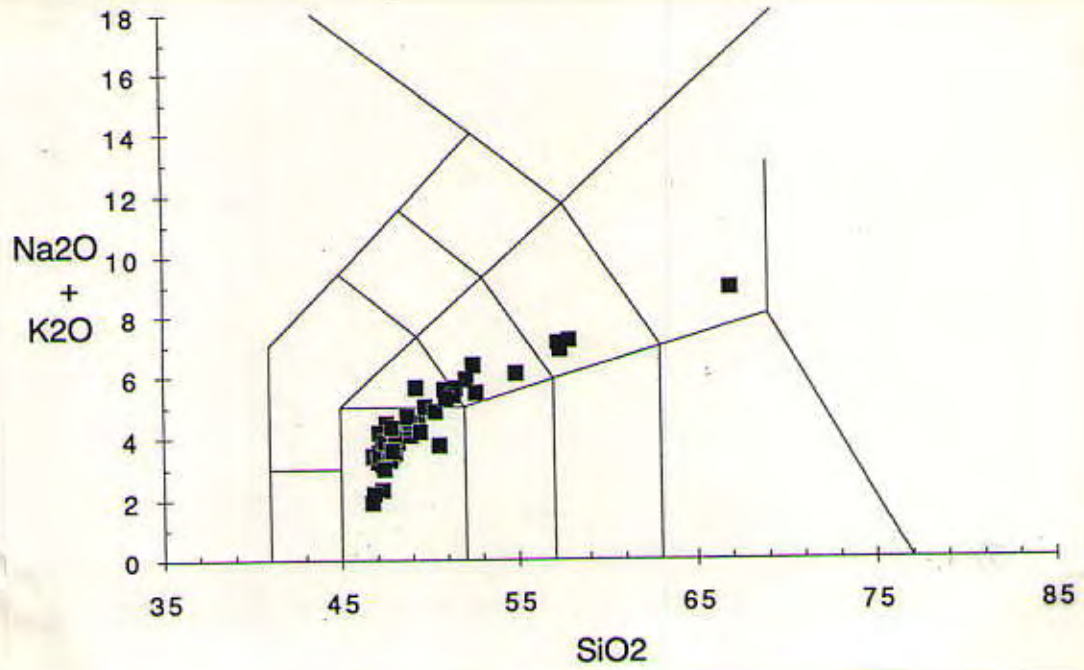


Figure 4.05(k)





Previous literature has classified alkalic rocks according to four different schemes (LeBas, et al., 1986; Macdonald and Katsura, 1964; Irvine and Baragar, 1972; Jakobsson, 1979). For the purposes of comparison among authors I have similarly displayed the data according to the four different classifications. These are shown in Figures 4.06, 4.07, 4.08, and 4.09. Figure 4.06 shows the silica vs. alkali IUGS Classification of Volcanic Rocks (LeBas, et al., 1986) on which the samples occupy the tholeiite basalt, trachybasalt, trachyandesite, and trachyrhyolite fields. Figure 4.07 shows the same thing as Figure 4.06 but with the Hawaiian alkalic/tholeiite line (Macdonald and Katsura, 1964). In this figure, all samples plot in the alkalic field except for Ey-17, STF-3, and Ey-49, which are olivine  $\pm$  clinopyroxene cumulates. Figure 4.08 shows an AFM (total alkalis, FeO, MgO) diagram with curves drawn for the tholeiitic and alkalic trends (Macdonald, Katsura, 1964). According to this plot, all Eyjafjöll samples lie within the two trends. Finally, Figure 4.09 shows a segment of the basalt tetrahedron (only samples with SiO<sub>2</sub> values less than 55 wt% were used) with nepheline, quartz, olivine, hypersthene (orthopyroxene) and diopside (clinopyroxene) components acquired from CIPW norm data, given in Appendix B. Jakobsson (1979) uses this tetrahedron for Icelandic volcanics as a means of distinguishing between alkalic (nepheline normative), transitional (no normative nepheline or quartz), and tholeiitic (quartz normative). Accordingly, the samples span the entire range from alkalic through transitional (the majority) to tholeiitic (one sample, Ey-30). Jakobsson (1972) was the first to characterize the neovolcanism in Iceland according to these guidelines. For the purpose of this investigation the samples will be considered to consist of several alkalic basalts, a large number of transitional basalts, and one tholeiite.



**Figure 4.06:** Eyjafjöll data according to the IUGS classification from LeBas et al. (1986). Data occupy the fields of tholeiitic basalt, trachybasalt, trachyandesite, and trachyrhyolite.



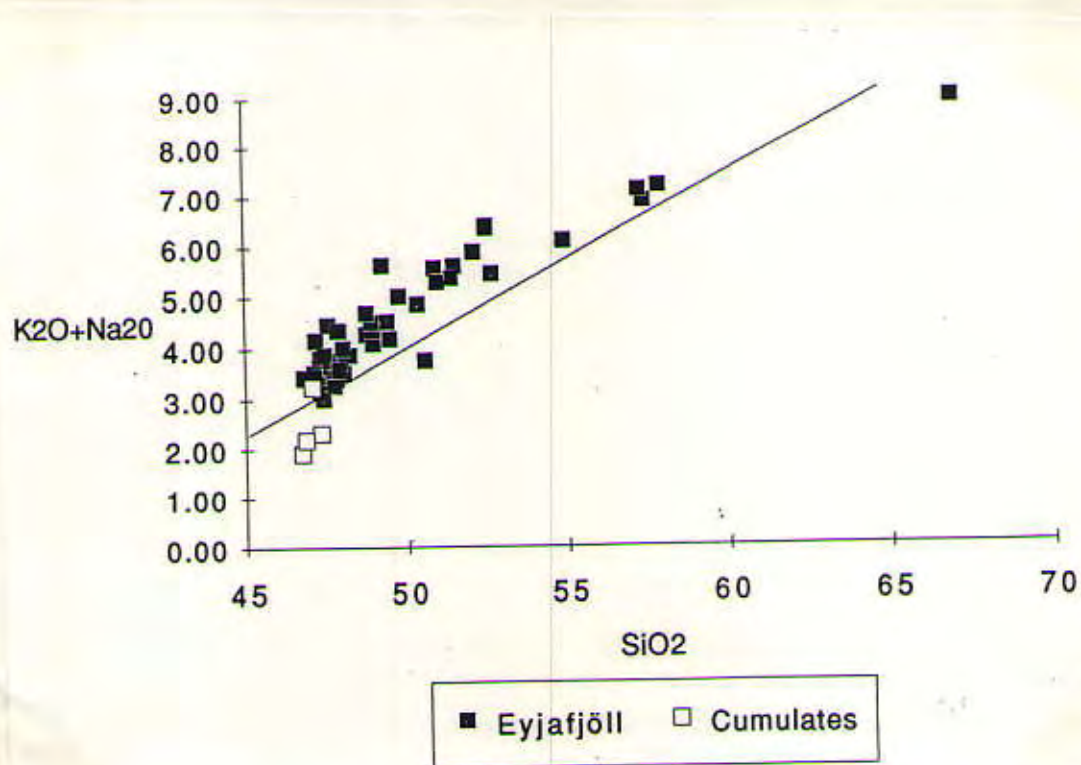


**Figure 4.07:** Alkali vs. silica diagram for Eyjafjöll samples. Line indicates Macdonald and Katsura (1964) division between tholeiitic and alkaline material. (Eyjafjöll data lie mainly in the alkaline field).

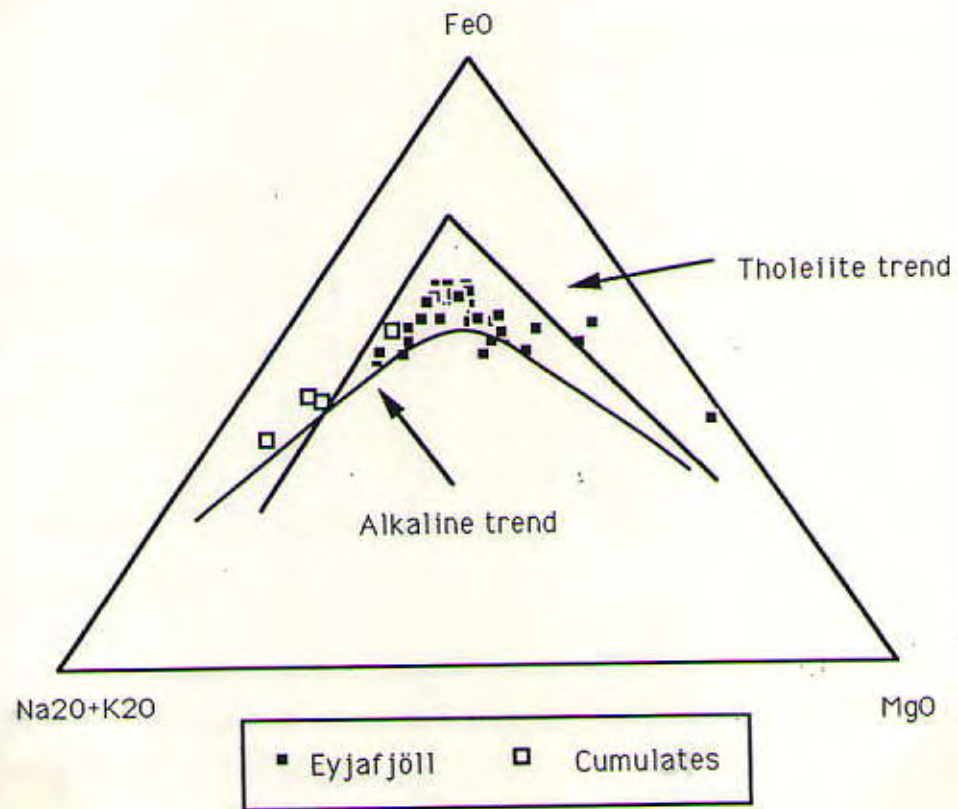


**Figure 4.08:** AFM diagram for Eyjafjöll data with tholeiite and alkaline trends from Irvine and Baragar (1972).



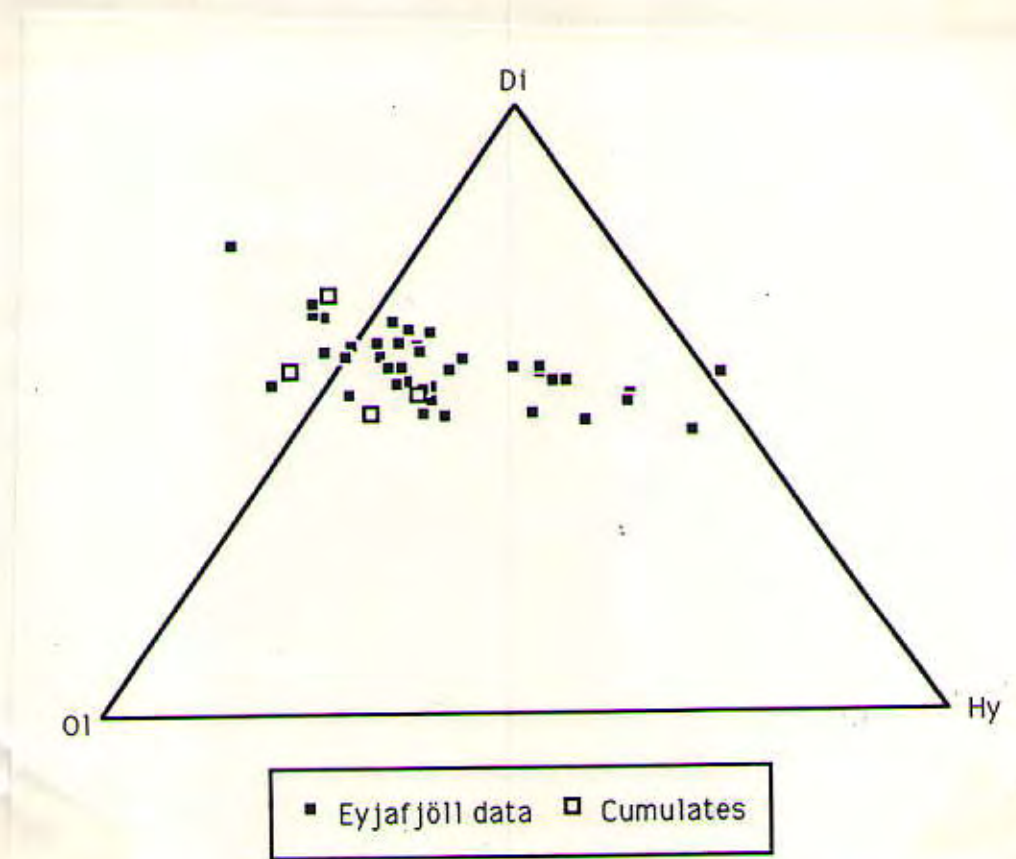


**Figure 4.09:** A segment of the basalt tetrahedron with Eyjafjöll data (all samples with  $\text{SiO}_2 < 55 \text{ wt\%}$ ).

In terms of whether or not there are any Fe-Ti basalts within this system, a definition has been used from Melson et al. (1976). According to this definition, Fe-Ti basalts have FeO contents higher than 12% and TiO<sub>2</sub> higher than 2%. Figure 4.10 shows how many of the Eyjafjöll rocks lie within this range.

Instrumental Neutron Activation Analysis (INAA) was used to obtain rare earth element concentrations, and Ta and Hf contents for seven samples. These are shown in Appendix B, and are displayed in Figure 4.11 as a chondrite-normalized rare earth element diagram. (Chondrite abundances come from Anders and Ebihara, 1982). As this figure shows, all samples have the same relative LREE enriched trends with the same parallel slopes. The only differences are in the absolute abundances. All samples are listed in the legend from bottom to top in order of decreasing MgO content (increasing evolution). All samples, except for Ey-4B show slight positive europium anomalies.

### **Petrography**

A summary of each thin section information is shown in Appendix C.

### **Groundmass**

Groundmass mineralogy consists of the following phases: plagioclase, titanomagnetite, clinopyroxene, apatite, ± olivine, ± glass. In rare instances, brownish colored (Mg-rich - picotite?) spinels are present in trace amounts (e.g., Ey-41). Plagioclase is always the most abundant crystal, ranging from 33 to 70%, averaging 50%. Olivine and clinopyroxene combined are the next most abundant, and in most cases are too small to differentiate. They range from 15 to 40% (combined abundance). Titanomagnetite averages 5-7%, and usually there is < 1% apatite. Glass is a minor phase, existing in only five



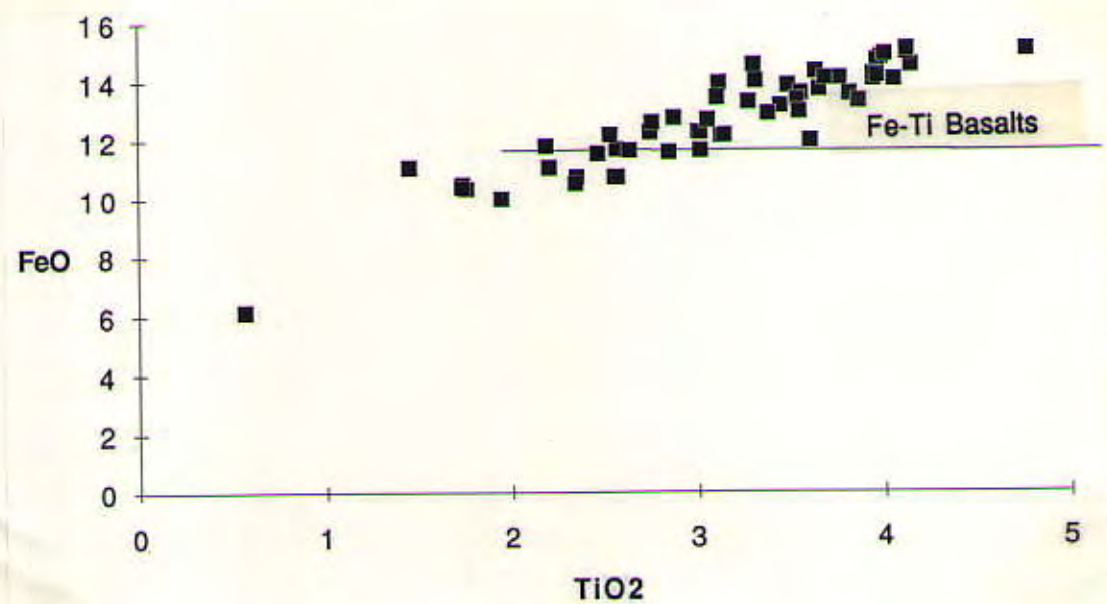


**Figure 4.10:** FeO vs. TiO<sub>2</sub> for all Eyjafjöll samples with SiO<sub>2</sub> < 55 wt%. Fe-Ti basalts are represented by samples with FeO > 12 wt% and TiO<sub>2</sub> > 2 wt%, all samples which lie above the black line.

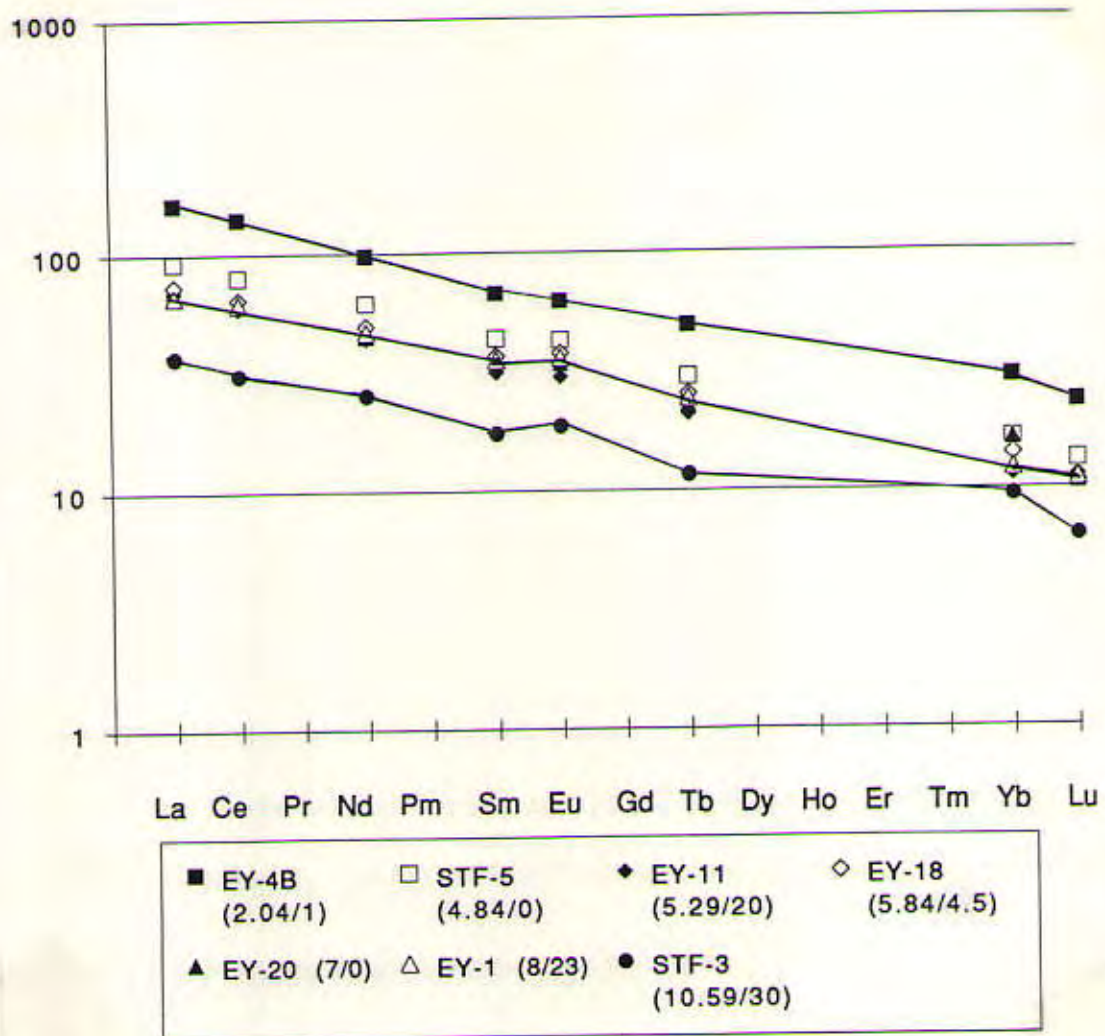


**Figure 4.11:** Chondrite-normalized REE patterns for Eyjafjöll samples. Numbers in parentheses refer to wt % MgO and % phenocrysts, in that order.



samples ( $\leq 15\%$ ), except for Ey-42 which has 75% glass.

Alteration minerals are present in nearly all samples, varying from 0-40%, with one sample, Ey-34 having 90% alteration. This alteration is usually characterized by greenish interstitial alteration, most likely chlorite and/or palagonite, and iddingsitized olivine crystals (rims mostly). In rare cases alteration is more extensive including significant chlorite and calcite, and occasionally even biotite.

Size of groundmass crystals (olivine, pyroxene, and titanomagnetite) ranges from 0.005 to 0.2 mm, with rounded, anhedral shapes; plagioclase crystals were always at least twice as large as the others, long and thin, and sub- to anhedral. Some samples show flow alignment of plagioclase feldspars in varying degrees, others none. Some samples show two different size ranges in the groundmass, perhaps signifying a change in cooling rate.

### **Vesicles**

Vesicles exist in 2/3 of the samples, varying in size from 0.05 to 10 mm, both within and among samples. Shapes range from rounded to irregular.

### **Phenocrysts**

Phenocrysts vary in abundance from 0% to 30%. They consist of olivine, clinopyroxene, plagioclase, and titanomagnetite. Nearly all phenocrysts show a variety of disequilibrium textures, including resorption, consertal growth with surrounding groundmass material, skeletal structure and embayment. Broken crystals are common. Frequently, within one rock there will be crystals of the same phase which represent every type of texture, in varying degrees of extent, (e.g., clean to frittered cores) suggesting multiple populations. (This was further assessed with microprobe work and is discussed in the next section).



Abundance of phenocrysts varies from sample to sample, but plagioclase is present as the most abundant crystal in almost all of the samples with Ey-1, Ey-17, Ey-19, Ey-49, and STF-3 as the only exceptions, (four of these are cumulate rocks (ankaramites), and the fifth, Ey-19 has only 3 to 4% phenocrysts). Clinopyroxene is the next most abundant phase, followed by olivine, and then titanomagnetite. Glomerocrysts of plagioclase and clinopyroxene are commonly present, and occasionally fragments (xenoliths) of clinopyroxene and olivine are found.

#### PLAGIOCLASE

Plagioclase crystals have the following textural characteristics: skeletal structure, resorption, embayment, frittered cores and/or rims, and broken crystals. Shapes vary from euhedral to anhedral. Combined with the zoning geometries seen within single crystals (Figure 4.12), these textures suggest disequilibrium and mixing. (A clean, euhedral, unzoned plagioclase was never seen).

Nearly every plagioclase crystal has opaque inclusions, often aligned linearly parallel to zoning (Figure 4.13). Clinopyroxene is also a common inclusion, and more rarely, olivine. Where large plagioclase crystals are found to include smaller plagioclase crystals it is described as synneusis, and thought to show evidence of agglomeration during growth, usually associated with active magma dynamics (Vance, 1969). Synneusis is found in nearly all samples as well.

Size of plagioclase crystals ranges from microphenocrysts (just slightly larger than the groundmass) to 6 mm. The large crystals are quite common.

#### CLINOPYROXENE

Clinopyroxene frequently shows disequilibrium textures; resorption and embayment are the most typical, though occasionally there are some skeletal



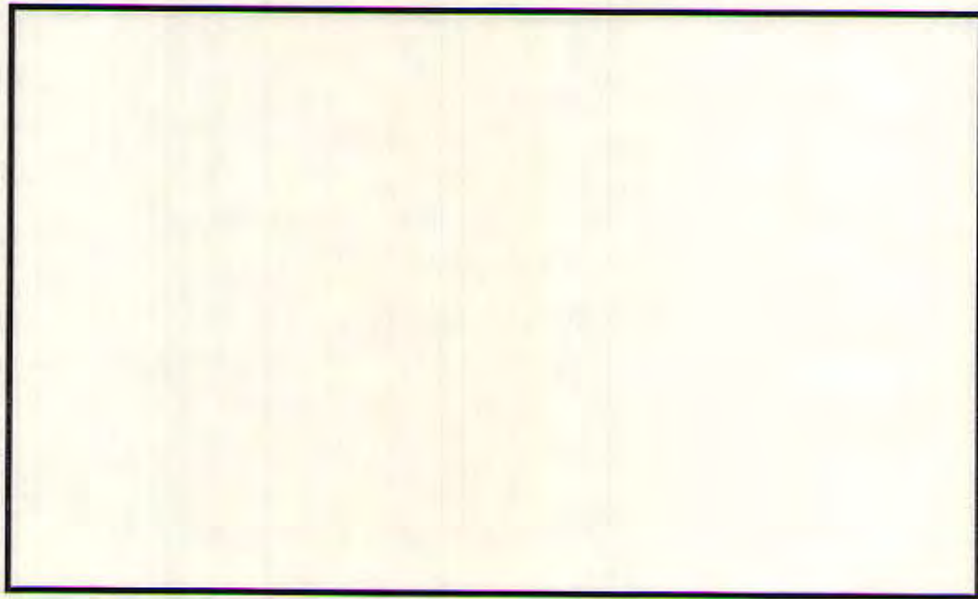


**Figure 4.12:** Thin section of Ey-10 showing plagioclase phenocryst with different zoning geometries (XPL). This same crystal was analyzed by microprobe, crossing from the core to the rim, a distance of 0.75 mm (Figure 4.15).

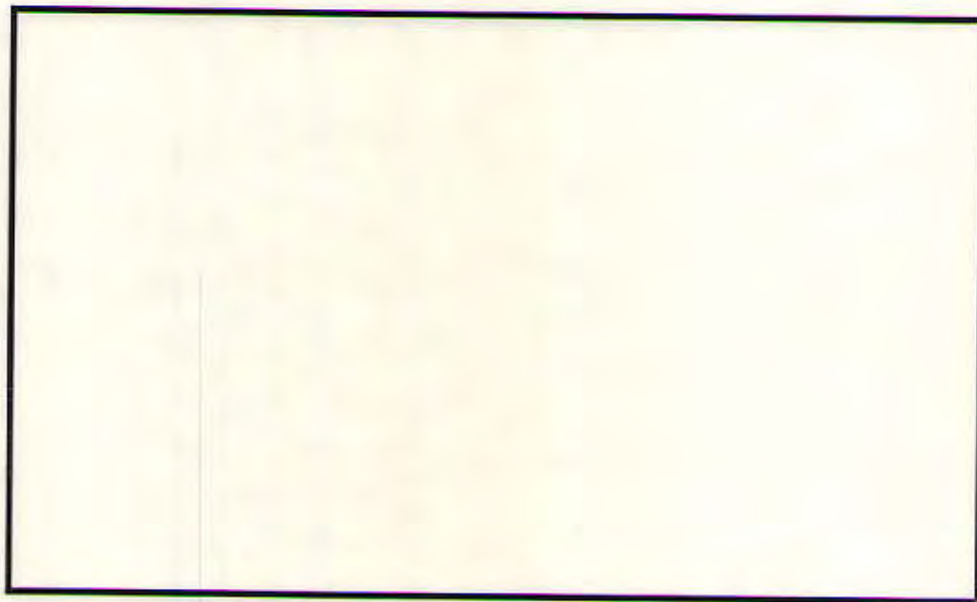


**Figure 4.13:** Thin section of Ey-29 showing plagioclase phenocryst with small clinopyroxene and opaque inclusions. The edges are embayed and slightly resorbed and the morphology appears almost skeletal at one end (PPL). The crystal is 2.5 mm long.



crystals, and rarely frittered cores. However, for every crystal with these disequilibrium textures there are about the same amount that are clean and euhedral. Size ranges from microphenocrysts to 13 mm. Inclusions are very common, and consist of opaques (most abundant), plagioclase (fairly common), and olivine (found in single phenocrysts in five different samples) (Figure 4.14).

#### OLIVINE

Olivine phenocrysts rarely show disequilibrium textures except for the cumulate rocks, where it is more common. These textures are similar as for the other phenocrysts, though never as extensive: skeletal structure, embayments and resorption. Frittered cores are very rare, but do occur. Iddingsitized rims are common.

Inclusions are rare in olivine. When they do exist they are opaque, usually rounded and varying in opacity from dark black to a brownish red. Work by other investigators (Baldrige et al., 1973) suggests that these might be picotite and/or chromite, as these are similarly found in other, nearby volcanic systems, including Vestmannæyar to the south and Hekla to the north. These Eyjafjöll inclusions vary in size but are usually  $< 0.1$  mm. A possible glass inclusion is found in one sample (unprobed) and is shown in Figure 4.15. Plagioclase is included in one olivine phenocryst in five different samples. Size of olivine phenocrysts varies from microphenocrysts to 10 mm.

#### TITANOMAGNETITE

Titanomagnetite is a rare phenocryst, existing in only 11 samples, and usually as a microphenocryst (just slightly larger than the groundmass), however they can get as large as 2.5 mm. It is difficult to distinguish textures for this phase as a transmitted light microscope was used for the petrography, but embayment and occasionally resorption were seen. A reflected microscope

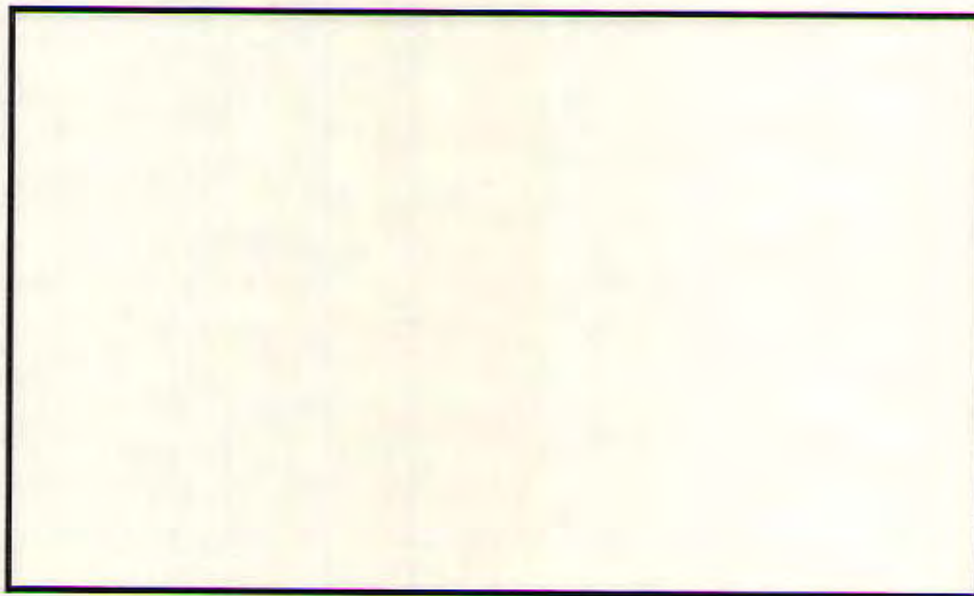


**Figure 4.14:** Thin section of Ey-39 showing two clinopyroxene phenocrysts growing together (PPL). There is a rounded olivine inclusion (0.5 mm across) in the right crystal and multiple opaque inclusions throughout.



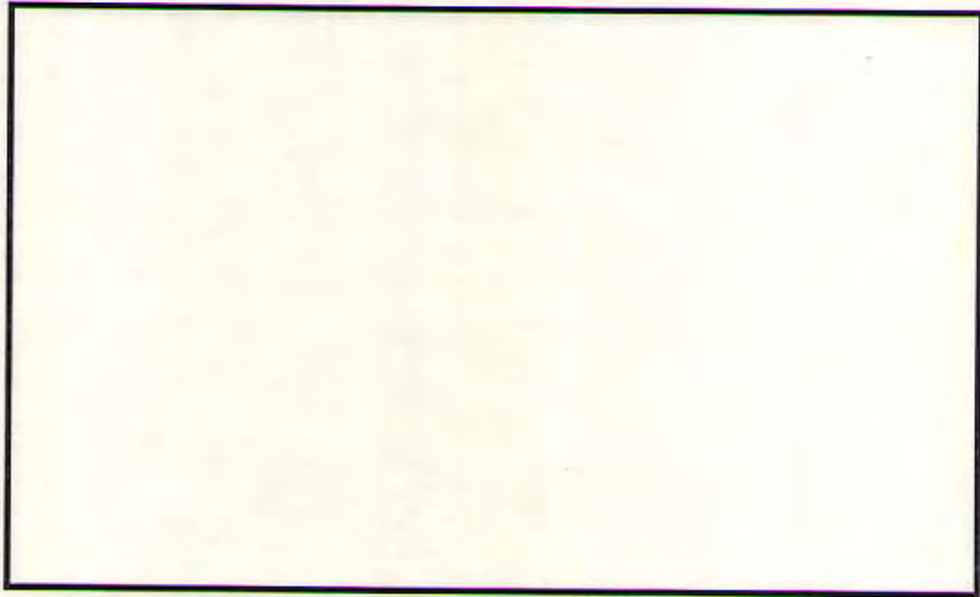


**Figure 4.15:** Thin section of Ey-36 showing olivine phenocryst with remnants of rounded glass inclusion (0.4 mm across). A large embayment is also visible (XPL).

was used prior to Microprobe analysis, with which significant zoning (subsolidus equilibrium) within these grains was seen. Those findings are discussed further in the next section.

#### CUMULATE ROCKS

There are four samples which have previously been referred to as ankaramites and/or cumulate rocks. They are characterized as cumulates based primarily upon their high abundance of phenocrysts, but also because they typically have high wt% MgO. (There are a few samples which are dominantly plagioclase phyric, 20 to 30% phenocrysts, and contain no olivine or clinopyroxene phenocrysts. These were, therefore not referred to as cumulates). These four 'cumulate' samples are Ey-1, Ey-17, Ey-49, and STF-3. Ey-1 has 20-25 % phenocrysts of which clinopyroxene is the most abundant followed by olivine and plagioclase (ankaramite). Ey-17 has 20% phenocrysts of which olivine is the most abundant followed quite closely by clinopyroxene (picrite basalt). Ey-49 has 25-30% phenocrysts of which olivine is the most abundant followed by clinopyroxene then plagioclase, in the ratio of 6:3:1 (ankaramite). STF-3 has 30% phenocrysts which consist of olivine, clinopyroxene, and plagioclase, all in equal proportions (ankaramite).

According to Irvine and Baragar (1971), a picrite basalt has normative olivine  $\geq 25\%$  and an ankaramite has a color index (normative ol + cpx + opx + ilm + mag)  $\geq (20 + (6/7)*(80-P))$ , where P = Anorthite composition of the normative plagioclase. Accordingly, among the Eyjafjöll samples, there are three ankaramites, and one picrite basalt. The geologic map of Eyjafjöll, Figure 4.02, refers to all cumulate rocks on Eyjafjöll as ankaramites regardless of their modal proportions. In this investigation I will use the term cumulate as a general description to be synonymous with ankaramite and/or picrite basalt since these rocks are full of large olivine and clinopyroxene (and



occasionally plagioclase) crystals, showing obvious mixing textures, and varying in modal proportions.

### **Mineral Compositions**

Samples of every phenocryst type were probed in order to combine the textural and compositional information, and define ranges. Full data is stored on the disk at the back of the thesis. These phenocrysts come from samples that represent the entire chemical range of Eyjafjöll data. Some are phenocryst rich (30%) , while others are aphyric. Compositions of most phases have large ranges within single samples showing multiple types of zoning (Table 4.02). It is important here to note that changes in composition of crystals from core to rim is dependent upon what part of the crystal was cut when making the thin sections. Therefore, all core compositions are minimums. Table 4.03 shows some representative analyses for clinopyroxene, and titanomagnetites along with a glass (hyaloclastite) composition.

#### **PLAGIOCLASE**

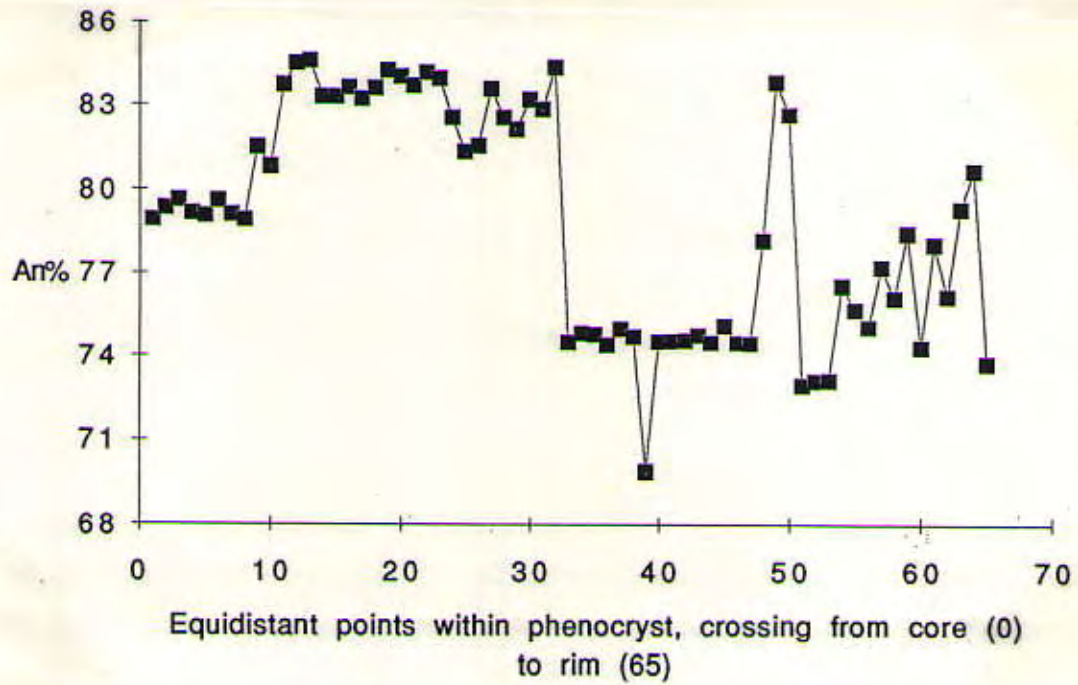
Nearly all plagioclase crystals show a large range in composition, with multiple populations present in all samples. Anorthite content ranges from An89 to An48 (Table 4.02). Compositional zoning is present as normal, reversed and oscillatory. This is shown best graphically, as the variation in composition of the crystal changes from rim to rim. A good example of oscillatory zoning is shown for a plagioclase crystal from sample Ey-10 (Figures 4.12, and 4.16). This crystal was probed with 65 equidistant points across an 0.75 mm distance from the core of the sample to the rim. Graphs of representative phenocrysts for all samples probed are given in Appendix D.

Table 4.02: Microprobe data.

Phenocrysts	Ey-1	Ey-3	Ey-4A	Ey-4B	Ey-10	Ey-17	Ey-20	STF-3
<b>Olivine</b>								
# probed	8	6	2		4	19	3	14
rim range	Fo61-Fo48	Fo70-Fo60	Fo57		Fo82-Fo76	Fo86-Fo76	Fo78-Fo70	Fo82-Fo55
core range	Fo83-Fo52	Fo82-Fo72	Fo82		Fo85-Fo75	Fo90-Fo81	Fo78	Fo88-Fo82
rim populations	61/56-48	whole range	one		82/79/76	whole range	whole range	whole range
core populations	81/65/58/51	whole range	one		85/81/75	90,86,82	78	88-82
zoning types	normal only	normal only	normal/none		n, r	n, r, o	normal	normal only
ave gm comp	Fo52	N/A	Fo53		N/A	N/A	N/A	Fo60-Fo55
<b>Plagioclase</b>								
# probed		7	5	6	21		6	11
rim range		An75-An53	An72-An42	An48-An32	An86-An55		An60-An50	An86-An51
core range		An82-An60	An80-An45	An48-An42	An86-An54		An64-An55	An86-An74
rim populations		whole range	72, 50-42	whole range	whole range		whole range	whole range
core populations		whole range	80,68,48-45	whole range	whole range		whole range	whole range
zoning types		n, r, o	normal only	n, r	n, r, o		n, r, o	n, r, o
ave gm comp		An57-An52	An42?	An32-An34?	An63-An54		An62-An55	An73-An51







**Figure 4.16:** Microprobe analysis from core to rim of a plagioclase phenocryst from Ey-10. This is the same crystal as shown in Figure 4.12.



## CLINOPYROXENE

Clinopyroxene phenocrysts display little variation, even among different samples (Figure 4.17). Three representative analyses are given in Table 4.03.

## OLIVINE

As with plagioclase, olivine phenocrysts have a large range in composition, with multiple populations present in all samples. Forsterite content ranges from Fo90 to Fo48 (Table 4.02). Compositional zoning is present as normal, reversed and oscillatory. This is shown best graphically, as the variation in composition of the crystal as one crosses from rim to rim. Graphs of representative phenocrysts for all samples probed are given in Appendix D.

## TITANOMAGNETITE

Titanomagnetite was looked at under reflected light microscopes prior to microprobe analysis in order to bring out the zoning. An example of this zoning is shown in Figure 4.18, where regions of ilmenite, magnetite and titanomagnetite are separated by differences in color. A pair of minerals (ilmenite and magnetite) was used to determine equilibrium temperatures and oxygen fugacity according to OXCALC (version 1.2 (1991): J.C. Stormer, Rice University). These results suggest temperatures and oxygen fugacities between the QFM and NNO buffers. This will be discussed in more detail in the next chapter. Table 4.03 gives magnetite and ilmenite pair compositions for Ey-4B and Ey-1. Ilmenite from this table represent separate regions within the crystal, while magnetite represents either fine beam analyses on separate magnetite regions, or wide beam analyses ("bulk" compositions) of zoned regions. These are referred to in the table as "fine beam" and "wide beam"

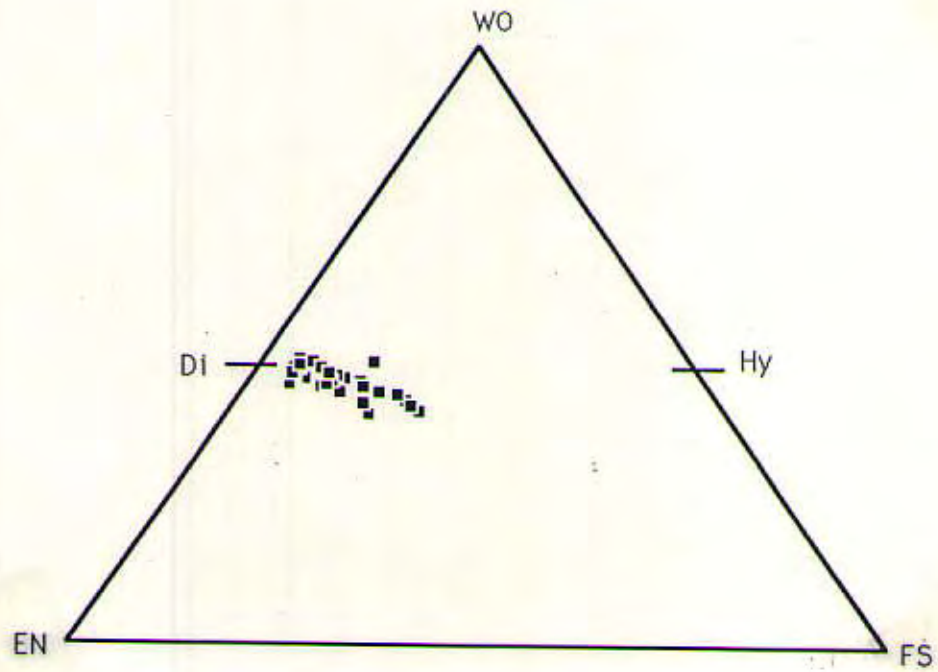


**Figure 4.17:** Pyroxene triangle showing averages of clinopyroxene phenocryst compositions for all Eyjafjöll samples.



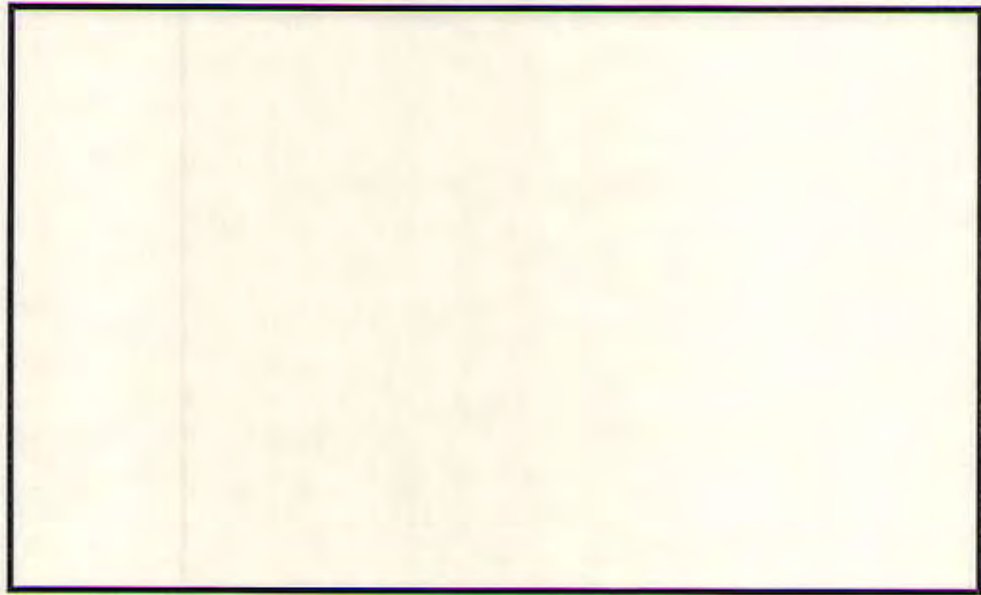


**Figure 4.18:** Thin section of Ey-1 showing titanomagnetite phenocryst (reflected light). The crystal is 0.5 mm wide and shows zoning of original titanomagnetite composition into regions of ilmenite and magnetite.

respectively.

#### GLASS

One hyaloclastite was probed, Ey-33, and multiple points were averaged for a representative composition (Table 4.03).

#### Isotopic Compositions

Only four samples were analyzed for He ratios (from olivine separates):

Sample #	R/Ra	Location/Description	Age
Ey-32	19.4±0.4	Hvammsmúli (picrite)	590±30
Ey-39	19.4±0.3	Seljalandsheiði (alkalic basalt)	<58±18
Ey-49	18.5±0.9	Asólfsskálaegg (ankaramite)	≈129±20
Ey-50	17.4±0.8	Asólfsskálaegg (alkalic basalt)	129±20